







# Cumulative Fraction of Response for Once- and Twice-Daily Delamanid in Patients with Pulmonary Multidrug-Resistant Tuberculosis

Suresh Mallikaarjun,<sup>a</sup> Moti L. Chapagain,<sup>b,c</sup> Tomohiro Sasaki,<sup>d</sup> Norimitsu Hariguchi,<sup>d</sup> Devyani Deshpande,<sup>b</sup>  
 Shashikant Srivastava,<sup>b,e</sup> Alexander Berg,<sup>f,\*</sup> Kuniko Hirota,<sup>d</sup> Yusuke Inoue,<sup>d</sup> Makoto Matsumoto,<sup>d</sup> Jeffrey Hafkin,<sup>a</sup>  
 Lawrence Geiter,<sup>a,\*</sup>  Xiaofeng Wang,<sup>a</sup>  Tawanda Gumbo,<sup>b,c</sup>  Yongge Liu<sup>a</sup>

<sup>a</sup>Otsuka Pharmaceutical Development & Commercialization, Inc., Rockville, Maryland, USA

<sup>b</sup>Baylor Research Institute, Dallas, Texas, USA

<sup>c</sup>Praedicare, Dallas, Texas, USA

<sup>d</sup>Otsuka Pharmaceutical Co., Ltd., Tokushima, Japan

<sup>e</sup>University of Texas Health Science Center, Tyler, Texas, USA

<sup>f</sup>Critical Path Institute, Tucson, Arizona, USA

**ABSTRACT** Pharmacokinetic (PK) and pharmacodynamic (PD) analyses were conducted to determine the cumulative fraction of response (CFR) for 100 mg twice-daily (BID) and 200 mg once-daily (QD) delamanid in patients with multidrug-resistant tuberculosis (MDR-TB), using a pharmacodynamic target (PDT) that achieves 80% of maximum efficacy. First, in the mouse model of chronic TB, the PK/PD index for delamanid efficacy was determined to be area under the drug concentration-time curve over 24 h divided by MIC ( $AUC_{0-24}/MIC$ ), with a PDT of 252. Second, in the hollow-fiber system model of tuberculosis, plasma-equivalent PDTs were identified as an  $AUC_{0-24}/MIC$  of 195 in log-phase bacteria and 201 in pH 5.8 cultures. Third, delamanid plasma  $AUC_{0-24}/MIC$  and sputum bacterial decline data from two early bactericidal activity trials identified a clinical PDT of  $AUC_{0-24}/MIC$  of 171. Finally, the CFRs for the currently approved 100-mg BID dose were determined to be above 95% in two MDR-TB clinical trials. The CFR for the 200-mg QD dose, evaluated in a trial in which delamanid was administered as 100 mg BID for 8 weeks plus 200 mg QD for 18 weeks, was 89.3% based on the mouse PDT and >90% on the other PDTs. QTcF (QTc interval corrected for heart rate by Fridericia's formula) prolongation was approximately 50% lower for the 200 mg QD dose than the 100 mg BID dose. In conclusion, while CFRs of 100 mg BID and 200 mg QD delamanid were close to or above 90% in patients with MDR-TB, more-convenient once-daily dosing of delamanid is feasible and likely to have less effect on QTcF prolongation.

**KEYWORDS** *Mycobacterium tuberculosis*, PK-PD index, PK-PD target, cumulative fraction of response, delamanid, hollow-fiber system model of tuberculosis

Worldwide, approximately 10 million people developed tuberculosis (TB) and 1.45 million (including those coinfecting with HIV) died of the disease in 2018, making it the leading cause of mortality from a single infectious agent and one of the top 10 causes of death overall (1). While drug-susceptible TB has a high cure rate following a standard 6-month regimen of antibiotics in controlled settings, global treatment success rates are 85% in routine patient care and, thus, are still not optimal (1). Management of multidrug-resistant TB (MDR-TB) is even more challenging. Accounting for approximately 460,000 cases per year worldwide, MDR-TB requires longer therapy with agents that are less effective (current rate of treatment success, 56%) and substantially more toxic (1). Additionally, resistance to either second-line injectables or fluoroquino-

**Citation** Mallikaarjun S, Chapagain ML, Sasaki T, Hariguchi N, Deshpande D, Srivastava S, Berg A, Hirota K, Inoue Y, Matsumoto M, Hafkin J, Geiter L, Wang X, Gumbo T, Liu Y. 2021. Cumulative fraction of response for once- and twice-daily delamanid in patients with pulmonary multidrug-resistant tuberculosis. *Antimicrob Agents Chemother* 65:e01207-20. <https://doi.org/10.1128/AAC.01207-20>.

**Copyright** © 2020 Mallikaarjun et al. This is an open-access article distributed under the terms of the [Creative Commons Attribution 4.0 International license](https://creativecommons.org/licenses/by/4.0/).

Address correspondence to Yongge Liu, [yongge.liu@otsuka-us.com](mailto:yongge.liu@otsuka-us.com).

\* Present address: Alexander Berg, Cognigen Corporation, Buffalo, New York, USA; Lawrence Geiter (independent consultant), Sunnt Isles Beach, Florida, USA.

For a companion article on this topic, see <https://doi.org/10.1128/AAC.01202-20>.

**Received** 12 June 2020

**Returned for modification** 15 July 2020

**Accepted** 13 October 2020

**Accepted manuscript posted online** 26 October 2020

**Published** 16 December 2020

lones (pre-extensively drug-resistant TB [pre-XDR-TB]) or to both (XDR-TB) reduces the success rate to a mere 39% (1). Thus, new therapies for effective and safe treatment of MDR-TB and XDR-TB are urgently needed.

Delamanid (Deltyba; Otsuka Pharmaceutical Co., Ltd., Tokyo, Japan) is a bicyclic nitroimidazooxazole compound that inhibits the synthesis of mycolic acids (2), key components of the lipid-rich cell wall of *Mycobacterium tuberculosis* (3). In preclinical studies, delamanid exhibited the lowest MIC among approved TB drugs against both drug-susceptible and drug-resistant isolates of *M. tuberculosis* (4) and demonstrated dose-dependent bactericidal effects in mice (2). In humans, two randomized, placebo-controlled trials assessed the efficacy and safety of delamanid plus an optimized background regimen (OBR) in the treatment of MDR-TB. In one study (trial 204; Table S5), patients who received delamanid with OBR had significantly higher sputum culture conversion (SCC) proportions after 2 months of therapy than those receiving placebo with OBR (45.4% versus 29.6%;  $P = 0.0083$ ) (5). In the second study (trial 213; Table S5), median time to SCC was numerically shorter in the delamanid/OBR arm (51 days) than in the placebo/OBR arm (57 days), although the difference did not reach the significance level of 0.05 ( $P = 0.0562$  for the comparison) (6). As of August 2020, delamanid is approved in 15 countries, including the European Union and Japan, as well as several high-TB-burden countries, including China, India, Indonesia, Peru, the Philippines, the Russian Federation, South Africa, and Ukraine, as part of an appropriate combination regimen for treatment of pulmonary MDR-TB in adults, when an effective treatment regimen cannot otherwise be composed for reasons of resistance or tolerability (7). The World Health Organization (WHO) has also recommended that delamanid be added to the WHO-recommended longer regimen in children and adolescents (6 to 17 years of age) with multidrug- or rifampin-resistant TB who are not eligible for the shorter MDR-TB regimen, under specific conditions (8).

For the treatment of infectious diseases, including TB, antibiotics should be dosed at concentrations that balance efficacy and safety. Currently, delamanid is approved at a dose of 100 mg twice daily (BID) (7) based on data from a number of clinical trials (5, 6, 9–11). A treatment regimen consisting of once-daily delamanid plus OBR has not been examined in isolation in clinical trials, but patients in trial 213 did receive 18 weeks of 200-mg once-daily (QD) dosing after 8 weeks of prior treatment with delamanid 100 mg delamanid twice a day (BID) (Table S5) (6). The present study was designed to determine the cumulative fraction of responses (CFRs) for 100 mg delamanid BID and 200 mg delamanid QD to compare the optimality of these two dosing regimens, thereby addressing the feasibility of once-daily administration of delamanid. Given the complexity of treatment regimens for MDR-TB, reducing the frequency of dosing via a once-daily regimen could have significant benefits for patient compliance, which in turn would be expected to improve outcomes for this difficult-to-treat infection.

## RESULTS

**PK/PD index and PK/PD target for delamanid in mice.** Pharmacokinetic (PK) parameters after the single administration of delamanid at doses of 0.625, 2.5, or 10 mg/kg in uninfected mice are shown in Table S1 for both plasma and lung tissue. Delamanid has a  $K_p$  (ratio of total concentration in tissue to that in plasma) value of 1.9 to 3 depending on the dose administered. Using a nonparametric superposition method, the single-dose plasma data were then used to estimate the plasma PK parameters after multiple-dose regimens, as shown in Table 1, that were used in an efficacy study (see below). The simulated PK profiles at the 4th week of a 4-week treatment for each individual regimen are shown in Fig. S2.

All tested delamanid dosing schedules significantly reduced bacterial burden as measured by  $\log_{10}$  CFU/lung compared to untreated controls, with a minimum of 1.672  $\log_{10}$  CFU/lung reduction by the 2.5 mg/kg once-weekly treatment and a maximum of 2.994  $\log_{10}$  CFU/lung reduction by the 10-mg/kg once-daily treatment (Table 1). As shown in Table 2 and Fig. 1, the inhibitory sigmoid maximum-effect ( $E_{max}$ ) model with a fixed Hill coefficient of 1.0 fitted the data well. The  $E_{max}$  of delamanid in mice was

**TABLE 1** Simulated PK parameters and observed bactericidal effects of various delamanid dosing regimens in *M. tuberculosis* Kurono-infected mice<sup>a</sup>

Regimen	Total cumulative dose (mg/kg)	AUC (mg · h/liter)			C <sub>max</sub> (mg/liter)	Log <sub>10</sub> CFU/lung	
		Weekly	0–24 h	%T <sub>&gt;MIC</sub>		Avg value (95% CI)	Avg reduction
10 mg/kg QD	280	97.272	13.896	100	1.184	4.138 (3.329–4.948)	2.994
2.5 mg/kg BID	140	56.752	8.107	100	0.437	4.301 (4.003–4.599)	2.831
10 mg/kg 3 times/wk	120	41.688	5.955	94.8	1.039	5.655 (3.860–5.450)	2.477
2.5 mg/kg QD	70	28.376	4.054	100	0.333	4.685 (4.162–5.208)	2.447
2.5 mg/kg 3 times/wk	30	12.161	1.737	74.6	0.301	5.126 (4.391–5.862)	2.006
10 mg/kg once/wk	40	13.896	1.985	37.3	1.012	5.199 (4.793–5.605)	1.933
0.625 mg/kg QD	17.5	9.18	1.311	100	0.11	5.447 (4.855–6.040)	1.685
2.5 mg/kg once/wk	10	4.054	0.579	24.7	0.297	5.460 (5.121–5.798)	1.672
No treatment	0	0	0	0	0	7.132 (5.763–8.501)	

<sup>a</sup>The total cumulative dose was for the 4-week treatment period. Weekly AUC, C<sub>max</sub>, and %T<sub>>MIC</sub> were estimated for the last week of the 4-week treatment period. The MIC was 0.012 mg/liter. AUC<sub>0–24</sub> is the average daily AUC of that week. The log<sub>10</sub> CFU/lung reduction was the average (n = 5, except for the regimen of 2.5 mg/kg three times per week, which had 4 mice due to the loss of one mouse resulting from a technical error) of the difference between the log<sub>10</sub> CFU value for each treatment group and the average (n = 5) for untreated mice at the end of the 4-week treatment period. For the three-times-per-week regimen, dosing was conducted on Mondays, Wednesdays, and Fridays. For the once-a-week dose regimen, dosing was conducted on Mondays. %T<sub>>MIC</sub>, percentage of time over the treatment period when delamanid remained above the MIC (0.012 mg/liter); weekly AUC, area under the delamanid concentration-time curve over 1 week of treatment during the last week of the 4-week treatment period; C<sub>max</sub>, maximal delamanid concentration.

estimated as a 2.96 log<sub>10</sub> CFU/lung reduction (95% confidence interval [CI], 2.63 to 3.29). The ratio of area under the concentration-time curve from 0 to 24 h to MIC (AUC<sub>0–24</sub>/MIC) was the pharmacokinetic-pharmacodynamic (PK/PD) parameter that best described delamanid efficacy (Pearson’s correlation coefficient = 0.97; P < 0.0001), while the percentage of time above the MIC (%T<sub>>MIC</sub>) exhibited moderate correlation (Spearman correlation coefficient = 0.53; P < 0.01). There was no significant correlation between efficacy and C<sub>max</sub>/MIC by Pearson’s correlation (P = 0.13). Additionally, inhibitory sigmoid E<sub>max</sub> modeling of log<sub>10</sub> CFU/lung reduction versus PK/PD exposure revealed corrected Akaike information criterion scores of 2.55 (r<sup>2</sup> = 0.99), 21.03 (r<sup>2</sup> = 0.86), and 22.07 (r<sup>2</sup> = 0.84) for AUC<sub>0–24</sub>/MIC, %T<sub>>MIC</sub>, and C<sub>max</sub>/MIC, respectively. This confirmed that AUC<sub>0–24</sub>/MIC was the parameter that best explained the delamanid antimicrobial effect. Therefore, the key PK/PD index driving delamanid efficacy was determined to be AUC<sub>0–24</sub>/MIC.

We then determined the pharmacodynamic target (PDT) for AUC<sub>0–24</sub>/MIC, using the AUC<sub>0–24</sub> value that achieved 80% of the E<sub>max</sub>, a cutoff that was used in previously published studies (12–16) and validated through the translation of HFS-TB data to clinical use for various TB drugs (as detailed in the Discussion). The PDT was an AUC<sub>0–24</sub>/MIC of 252 (95% CI, 139 to 649) (a plasma AUC<sub>0–24</sub> of 3.021 mg · h/liter divided by an MIC of 0.012 mg/liter for the *M. tuberculosis* strain used in the study), which achieved a 2.36 log<sub>10</sub> CFU/lung reduction from the untreated control.

**PDT for delamanid from HFS-TB.** The delamanid MIC of strain H37Rv, which was used in the study of the hollow-fiber system model for TB (HFS-TB), was determined to be 0.015 mg/liter. Maximal killing by delamanid of bacteria in log-phase growth and growth at pH 5.8 was recorded on day 7, after which all regimens failed as bacterial regrowth occurred. This regrowth in the HFS-TB has been observed for all TB drugs in

**TABLE 2** Inhibitory sigmoid E<sub>max</sub> parameters for delamanid AUC<sub>0–24</sub>/MIC from mouse and HFS studies and human EBA trials<sup>a</sup>

Study type	Estimate (95% CI) of best-fit value of:			
	E <sub>max</sub> (log <sub>10</sub> CFU)	Hill coefficient	EC <sub>50</sub> (AUC <sub>0–24</sub> /MIC)	EC <sub>80</sub> (AUC <sub>0–24</sub> /MIC)
Mouse	2.96 (2.63–3.28)	1 (fixed) (NE)	63 (40–99)	252 (139–649)
HFS				
Log-phase growth	1.49 (1.26–1.82)	1.86 (1.16–3.16)	240 (171–369)	506 (306–777)
pH 5.8 culture	2.35 (1.90–2.79)	1.5 (imprecise)	207 (87–361)	522 (210–910)
Human EBA	0.626 (0.448–0.835)	4.39 (1.30–8.14)	125 (57.9–213)	171 (79.0–292)

<sup>a</sup>E<sub>max</sub>, maximum killing from time-matched untreated controls in the mouse and HFS studies or from baseline in the EBA trials; EC<sub>50</sub> and EC<sub>80</sub>, AUC<sub>0–24</sub>/MIC required for 50% and 80% of E<sub>max</sub>, respectively; NE, not estimated.

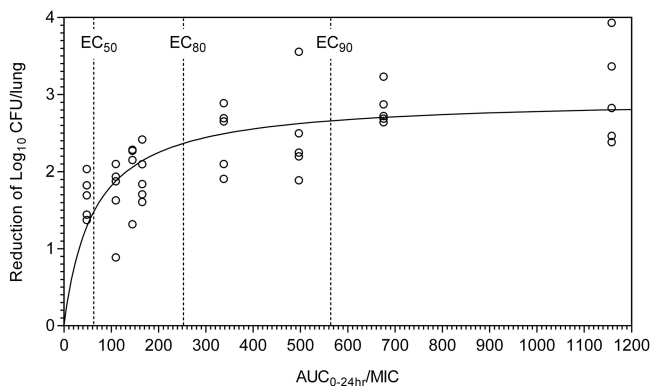


**FIG 1**  $\text{Log}_{10}$  CFU/lung reduction by  $\text{AUC}_{0-24}/\text{MIC}$  in mice. Each circle represents data from an individual mouse. The reduction was the difference between  $\text{log}_{10}$  CFU per lung in the treated mouse and the average value for the untreated mice. Multiple-dose  $\text{AUC}_{0-24}$  was simulated from single-dose PK data.  $\text{EC}_{50}$ ,  $\text{EC}_{80}$ , and  $\text{EC}_{90}$  represent the  $\text{AUC}_{0-24}/\text{MIC}$  to achieve 50%, 80%, and 90% of the maximum efficacy, respectively.

monotherapy, including rifampin (17) and isoniazid (18), the two most important first-line TB drugs. The regrowth in the HFS-TB has been attributed to the emergence of resistance under monotherapy. Therefore, the killing (as calculated by the reduction of  $\text{log}_{10}$  CFU per milliliter in the delamanid treatment arms from the time-matched untreated control) at day 7 was used in the inhibitory sigmoid  $E_{\text{max}}$  model, as shown in Table 2 and Fig. 2.  $\text{AUC}_{0-24}$  and average  $\text{log}_{10}$  CFU-per-milliliter data for each regimen at day 7 can be found in Table S3 (for log-phase growth) and Table S4 (for growth at pH 5.8).

The  $\text{EC}_{80}$  (80% of the  $E_{\text{max}}$ ) values derived on day 7 were  $\text{AUC}_{0-24}/\text{MIC}$  ratios of 506 (95% CI, 360 to 777) for log-phase growth and 522 (95% CI, 210 to 910) for growth at pH 5.8. PDTs obtained in the HFS-TB corresponded to the drug AUCs at the site of infection (i.e., lung), while the PK/PD analyses of animal and human data were based on the plasma levels. However, there are no human data on delamanid lung penetration and the relative ratio of AUC in lung versus plasma. Hence, the  $K_p$  value could only be inferred from animal data at this time. As shown Table S1, delamanid  $K_p$  values were 1.9, 2.9, and 3.0 when delamanid was administered as a single dose at 0.625, 2.5, and 10 mg/kg, respectively. Further, it was previously shown that after a single administration of delamanid at 3 mg/kg, the  $K_p$  was 2.4 ( $\text{AUC}_{0-24} = 13.768 \text{ mg} \cdot \text{h}/\text{kg}$  in lung versus  $5.673 \text{ mg} \cdot \text{h}/\text{liter}$  in plasma) in mice (19). Using the average of 2.6 of the 4 mouse  $K_p$  values of 1.9, 2.4, 2.9, and 3, the plasma-equivalent PDTs for log-phase growth and

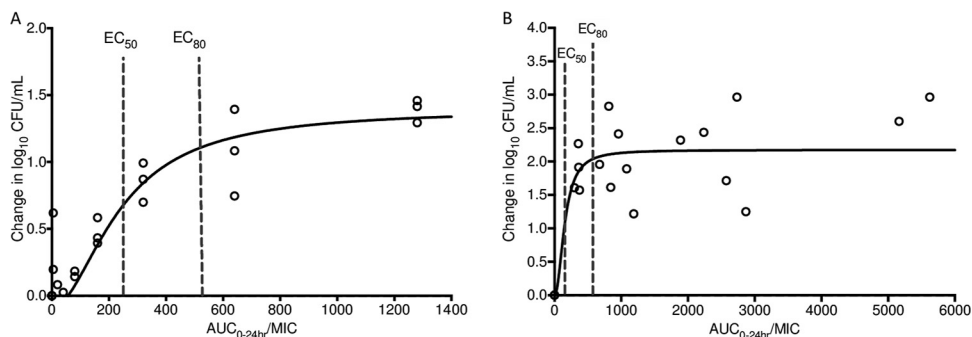


**FIG 2** Inhibitory sigmoid  $E_{\text{max}}$  model for log-phase growth (A) and growth at pH 5.8 (B). An inhibitory sigmoid  $E_{\text{max}}$  model was used to examine the  $\text{log}_{10}$  CFU-per-milliliter values for day 7 as the response variable versus  $\text{AUC}_{0-24}/\text{MIC}$  from various regimens. (A) Each circle represents data from one HFS-TB with targeted  $\text{AUC}_{0-24}/\text{MIC}$ . (B) Each circle represents data from one HFS-TB with observed  $\text{AUC}_{0-24}/\text{MIC}$ .  $\text{EC}_{50}$  and  $\text{EC}_{80}$  represent the  $\text{AUC}_{0-24}/\text{MIC}$  to achieve 50% and 80% of the maximum efficacy, respectively.

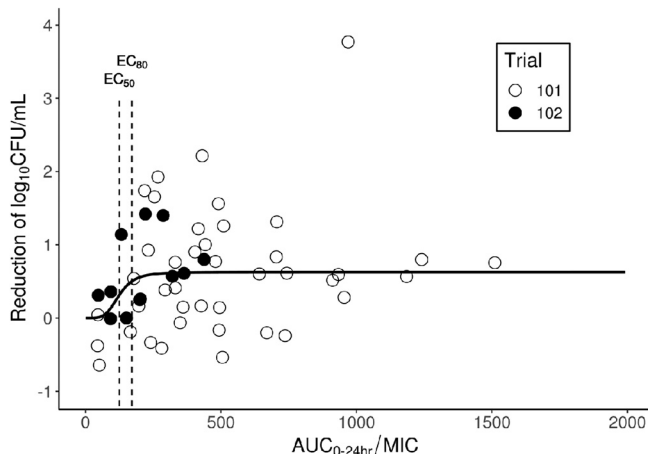


**FIG 3** Sputum log<sub>10</sub> CFU reduction from baseline (prior to the start of treatment) to the end of treatment and AUC<sub>0-24</sub>/MIC relationship in trial 101 and trial 102. Each circle represents data from one patient. AUC<sub>0-24</sub> is the daily area under the concentration-time curve on day 14 (trial 101) or day 7 (trial 102); EC<sub>50</sub> and EC<sub>80</sub> represent the AUC<sub>0-24</sub>/MIC to achieve 50% and 80% of the maximum efficacy, respectively.

growth at pH 5.8 were 195 (95% CI, 139 to 299) and 201 (95% CI, 81 to 350), respectively.

**PDT for delamanid in humans.** Individual delamanid AUC<sub>0-24</sub>/MIC and sputum culture bacterial burden reduction data from two early bactericidal activity (EBA) trials in drug-susceptible TB patients are shown in Table S6. The relationship between the reduction of log<sub>10</sub> CFU per milliliter from baseline and AUC<sub>0-24</sub>/MIC was modeled using a nonlinear mixed-effect approach to assess the PDT of delamanid in humans. As shown in Fig. 3, an inhibitory sigmoid *E<sub>max</sub>* model of bactericidal activity and plasma AUC<sub>0-24</sub>/MIC with random effect on maximum inhibition (*I<sub>max</sub>*) provided the best fit and was selected as the final model. Parameter estimates are summarized in Table 2. Goodness of fit and visual predictive check plots are provided in Fig. S4 and S5, respectively. The plasma AUC<sub>0-24</sub>/MIC producing 80% inhibition (i.e., the PDT) was calculated to be 171 (95% CI, 79 to 292).

**CFR in patients with MDR-TB who were treated with 100 mg delamanid BID or 200 mg delamanid QD.** As shown in Table 3, when patients were treated with 100 mg delamanid BID, the observed CFR was 100% in the trial 204 study population and ≥95% in the trial 213 study population, regardless of which PDT was used in the calculation. The CFR for 200 mg delamanid QD was 89.3% using the mouse PDT and above 90% for the other three PDTs in the trial 213 population.

**QTcF prolongation.** In trial 213, patients with MDR-TB received 100 mg delamanid BID for 8 weeks, followed by 200 mg QD for 18 weeks (Table S5), thus providing an opportunity to compare the magnitude of corrected QT (QTc) interval prolongation

**TABLE 3** Cumulative fraction of response following 100-mg BID or 200-mg QD delamanid dosing<sup>a</sup>

Study type	Plasma-equivalent PDT (AUC <sub>0-24</sub> /MIC)	CFR for population and dosage		
		Trial 204, 100 mg BID (n = 104)	Trial 213, 100 mg BID (n = 246)	Trial 213, 200 mg QD (n = 246)
Mouse	252	100	95.9	89.3
HFS				
Log-phase growth	195 <sup>b</sup>	100	98.0	93.4
pH 5.8 culture	201 <sup>b</sup>	100	98.0	91.7
Human EBA	171	100	98.0	95.9

<sup>a</sup>BID, twice daily; CFR, cumulative fraction of response; EBA, early bactericidal activity; HFS-TB, hollow-fiber system model of tuberculosis; n, number of patients; PDT, pharmacodynamic target; QD, once daily.

<sup>b</sup>Plasma-equivalent PDT for the HFS-TB study was calculated by dividing the HFS-TB PDT with the mouse *K<sub>p</sub>*.

under the two different dosing regimens. As shown previously, the mean differences from baseline in QTcF (QTc interval corrected for heart rate by Fridericia's formula) between the delamanid-plus-OBR group ( $n = 341$ ) and the placebo-plus-OBR group ( $n = 170$ ) after 8 weeks of treatment with the 100-mg BID dose was 5.3 ms (90% CI, 2.8 to 7.9 ms) compared with 2.5 ms (90% CI,  $-0.3$  to 5.3 ms) at the end of 18 weeks of treatment with the 200-mg QD dose (6). Thus, the QTc interval prolongation associated with 200-mg QD dosing was about 50% of that seen with 100-mg BID dosing.

## DISCUSSION

The process to develop TB drugs is highly laborious due to the complexity of TB pathology, the spatial and temporal heterogeneity of TB lesions, which drives variable microbial killing and resistance emergence, and the lack of real-time biomarkers to measure treatment outcomes (20, 21). Delamanid was identified using *in vitro* and animal TB models that demonstrated bactericidal effects on replicating, dormant, and intracellular bacilli (22). Clinical development involved the traditional drug development pathway of testing on healthy subjects first, followed by proof-of-concept and dose selection phase II trials and a phase III trial in TB patients (22). In the EBA (phase IIa) trials, 200-mg QD and 300-mg QD doses of delamanid monotherapy appeared to produce similar bactericidal activity following 14 days of treatment in patients with drug-susceptible pulmonary TB (23). Nonetheless, due to observed delamanid dose-limiting absorption (23), the phase IIb trial used BID dosing. In the trial, 100 mg BID and 200 mg BID demonstrated similar proportions of sputum culture conversion after 8 weeks of treatment when added to an OBR in pulmonary MDR-TB patients (5). Therefore, the 100-mg BID dose regimen was subsequently approved by regulatory agencies, first in 2014 by the European Medicines Agency (EMA) (22). However, insufficient data were available for a thorough PK/PD analysis of delamanid at that time, including exploring alternate dosing regimens.

In the multipronged PK/PD analyses presented here, we attempted to understand the relationship between the PK and PD of delamanid using nonclinical and human PK/PD data, based on the principles outlined in a guideline from the EMA on the use of PK/PD in the development of antimicrobial medicinal products (24). Such principles are also consistent with the FDA guidance (25) for developing antibiotics and the methodology of establishing appropriate doses for TB drugs from the WHO (26). In addition to using data from the mouse model and human EBA trials, we utilized the data from the HFS-TB model, which was recently qualified by the EMA as a method for use in support of selection and development of antituberculosis drugs (27) and is supported by the FDA as a complementary tool for dose selection (28, 29). The HFS-TB is an *in vitro* system that can mimic human PK characteristics of antimycobacterial drugs at the site of infection and was built for the purpose of exploring the concentration-effect relationships potentially relevant to the treatment of TB. Another merit of the HFS-TB is that drug efficacy can be examined under different growth conditions of *M. tuberculosis* bacilli (log-phase growth and low pH to simulate a slowly replicating state) and, thus, may capture some of the microbial heterogeneity of TB lesions. In addition, repetitive sampling in the HFS-TB, as in patients' sputum, allows determination of several quantitative PD measures, including kill slopes.

$AUC_{0-24}/MIC$  is the PK/PD index for delamanid, as determined in the mouse study. In the PDT and CFR calculations,  $AUC_{0-24}$  was obtained using noncompartmental methods for data from the mouse TB model, EBA trials (trials 101 and 102), and trial 204. For the data from the HFS and trial 213, model-based approaches were applied to obtain  $AUC_{0-24}$ . As shown in Fig. S3 for the HFS and the companion article (30) for trial 213, the model predictions are reasonably consistent with observations. Thus, we determined that the calculated AUCs were accurate and could be used here for PK/PD analyses. The MICs of the infecting strains used in the mouse study (MIC of 0.012 mg/liter) and the HFS-TB study (MIC of 0.015 mg/liter) are in the range of the MICs in the EBA studies (0.006 mg/liter to 0.05 mg/liter) (Table S6 and Table S7) and trial 204 (0.001

to 0.05 mg/liter) (4). The individual MICs from trial 213 have not been published, but the distribution is similar to that in trial 204.

In our PK/PD analyses, two critical cutoff values were used:  $EC_{80}$  (80% of the  $E_{max}$ ) and 90% for CFR. There is no regulatory or industry standard for a set percentage of the  $E_{max}$  to determine PDT. Since the  $E_{max}$  in the inhibitory sigmoid maximal microbial kill model is on an asymptote, a percentage of the  $E_{max}$  needs to be selected for the purpose of determining the PDT. Traditionally in the drug development industry, 80% or 90% of  $E_{max}$  has been selected (13, 31). We selected  $EC_{80}$  in our study based on 3 pieces of validation work that showed that at the level of 80%, PDTs selected from HFS-TB studies reliably predicted the drug exposures associated with clinical success. First, the accuracy to forecast optimal exposures and breakpoints in patients with TB using the  $EC_{80}$ -based findings from the HFS-TB was validated by examining 20 clinical studies that were published after 26 HFS-TB experiments had been published (12). The HFS-TB  $EC_{80}$ -based PDT predicted optimal drug exposures and doses that were identified in these 20 clinical studies based on agnostic machine learning analyses. The predictive accuracy of the HFS-TB in forecasting the clinical exposure values was 94.4% (95% CI, 84.3% to 99.9%). Second, a systematic analysis of HFS-TB and clinical findings indicated that  $EC_{80}$ -based findings in tandem with Monte Carlo simulations for attainment of that target were similar between patients and the preclinical model (32). Third, a comprehensive analysis of all preclinical PK/PD studies in TB with clinical comparisons concluded that PDTs using 80% of  $E_{max}$  obtained in preclinical studies provided a reliable predictor of clinical success (31).

Importantly, increasing the efficacy level from 80% to 90% requires a large increase of  $AUC_{0-24}$ , since the efficacy curve is flat from  $EC_{80}$  and above (i.e., on an asymptote). In our mouse model, the increase from  $EC_{80}$  to  $EC_{90}$  (only an additional 0.3  $\log_{10}$  CFU reduction) requires the increase of  $AUC_{0-24}/MIC$  from 252 to 566 ( $AUC_{0-24}$  increases from 3.021 to 6.797 mg · h/liter) (Fig. 1), which represents very little gain in terms of microbial killing for a 2.2-fold jump in needed AUC. Doubling the  $AUC_{0-24}$  in humans from the 100-mg BID delamanid dose will likely increase side effects, such as the QTc interval prolongation. Therefore, taking into consideration the balance between efficacy and safety, we selected  $EC_{80}$  in this study. As for the cutoff of CFR, the EMA guidance provides 90% as an appropriate level for PK/PD analysis (24). FDA does not define a cutoff value for CFR as far as we are aware. However, it is generally accepted that the goal for PTA (probability of target attainment) or CFR should be at least 90% (33, 34). A white paper published in 2017 assessed the relationship between the PTA for antibacterial dosing regimens and FDA approval and concluded that, among the programs evaluated, FDA approval was granted for 88% of those achieving at least a 90% PTA versus much lower approval rates for development programs using lower percentages of PTA (35). Therefore, we felt that  $EC_{80}$  and CFR at 90% were reasonable selections for our PK/PD analyses.

We showed that the plasma or plasma-equivalent PDTs ( $AUC_{0-24}/MIC$ ) for delamanid ranged from 171, obtained from the human EBA trials, to 252, obtained in the mouse TB model. The PDTs from the HFS-TB assessments were 195 in log-phase growth and 201 in growth at pH 5.8. The values are within a narrow range, considering the very different models used to determine PDTs. Importantly, regardless of which PDT was used, the CFRs were >95% for the 100-mg BID dose, the dose currently approved for the treatment of pulmonary MDR-TB in adults, strongly indicating that this dose is appropriate to achieve the PDT. The similarity of the efficacy of the 200-mg BID dose evaluated in trial 204 to that of the 100-mg BID dose (5) is consistent with this conclusion.

While our analysis indicates that the 100-mg BID dose of delamanid can achieve  $EC_{80}$  in more than 90% of the patients, once-daily dosing of delamanid would be more convenient for patients and could lead to enhanced adherence. Our data show that the 200-mg QD dose could produce CFRs close to or above 90%, suggesting that 200 mg QD may be a feasible option for the MDR-TB population we evaluated. Furthermore, 200 mg QD likely causes less QTc interval prolongation than the 100-mg BID regimen,

as shown in trial 213. To date, QTc interval prolongation is the major safety concern for delamanid.

The CFRs achieved with 200 mg delamanid QD are slightly lower than those from the 100-mg BID dose, and thus, once-daily doses higher than 200 mg could be explored. Data on once-daily delamanid doses higher than 200 mg, such as 300 mg, have been studied in healthy subjects, as well as in a 14-day EBA trial in pulmonary TB patients (23). In the EBA study,  $C_{max}$  and AUC values for 300 mg QD were higher than those for 200 mg QD but still below those achieved with the 100-mg BID dose (5). Based on delamanid exposure, QTc interval prolongation from the 300 mg QD dose would be expected to be lower than that from the 100 mg BID dose, since the concentrations of both delamanid and DM-6705, a major metabolite causing QTc interval prolongation, are lower following the 300-mg QD dose than the 100-mg BID dose (7).

Our study has several limitations. First, the mouse multiple-dose PK profiles were simulated from single-dose data in healthy animals. However, PK parameters obtained using this method were similar to the actual measurements obtained with multiple doses of delamanid in *M. tuberculosis* Kurono-infected mice at the dose of 2.5 mg/kg and when using the one-compartment model method (see Table S2 and the other supplemental material). Thus, the nonparametric superposition method provided a reasonable estimation of the PK parameters following multiple doses of delamanid in this study. Further, delamanid PK parameters were similar between healthy subjects and patients with TB (7). Second, different phenotypes of TB bacilli (i.e., replicating, and dormant) respond differently to drug treatment, and animal models used to generate PK/PD measures of efficacy may not faithfully mimic TB disease in humans. It should be noted, however, that the HFS-TB examined low-pH conditions, which is thought to mimic certain caseous TB lesions (36–40). Third, the mouse and HFS-TB studies were designed to evaluate bactericidal activity and not sterilizing efficacy and relapse prevention of the drug. Fourth, as shown in Fig. 3, human EBA responses in trials 101 and 102 were variable. However, the model described well the central tendency values based on goodness of fit and visual predictive check (Fig. S4 and S5). Fifth, since no human lung tissue drug concentration data are available for delamanid, we used the lung tissue and plasma levels in a mouse study to calculate  $K_p$  and obtain the plasma-equivalent HFS-TB PDT. In a separate study using guinea pigs, the  $K_p$  was 18.4 (41), which would make the plasma equivalent PDT much lower. Since human TB lesions are heterogenous, TB drug penetrations are likely lesion type dependent (42). Future studies using animals and, ideally, human TB lungs are needed to investigate delamanid lesion penetration. Finally, the nonclinical PDTs were determined with monotherapy and the human PDT was determined from short-term monotherapy in EBA trials; therefore, we cannot exclude the possibility that PDTs for each drug component in a multidrug regimen when used for MDR-TB patients could be different.

In conclusion, in the present study, we identified  $AUC_{0-24}/MIC$  as the index of delamanid efficacy. Using PDTs obtained from different models, we further showed that delamanid at 100 mg BID and 200 mg QD achieved cumulative fractions of response of  $\geq 90\%$  in two large trials of patients with pulmonary MDR-TB. Therefore, once-daily doses of delamanid, such as 200 mg or higher, may be possible options, likely with less QTc interval prolongation than with the 100-mg BID dose. Hence, QD doses of delamanid should be further evaluated in future clinical trials.

## MATERIALS AND METHODS

**General approach to the PK/PD analysis.** To determine CFR for the 100-mg BID and 200-mg QD doses of delamanid, we used general principles for PK/PD analysis as outlined in several publications, including one from the EMA (24, 26, 33). We used data from a mouse and an HFS-TB study and several human trials for this effort (Table S5). The steps taken to obtain the CFRs are outlined in Fig. S1.

**Materials.** *M. tuberculosis* Kurono (ATCC 35812) was used in the mouse infection model, and H37Rv (ATCC 27294) was used in the HFS-TB studies. SLC:ICR mice were obtained from Japan SLC, Inc. (Hamamatsu, Shizuoka, Japan). The hollow-fiber cartridges with polysulfone hollow fibers were purchased from FiberCell System, Inc. (New Market, MD, USA). Delamanid was supplied by Otsuka Pharmaceutical Co., Ltd. (Tokushima, Japan).



**PK analysis of single-dose delamanid in mice and estimation after multiple doses.** All animal studies were carried out in accordance with the document “Guidelines for Animal Care and Use in Otsuka Pharmaceutical Co., Ltd.” To evaluate delamanid PK, uninfected SLC:ICR mice were administered a single dose of delamanid at 0.625, 2.5, or 10 mg/kg by oral gavage. Three to six mice in each dosage group were sacrificed at 1, 2, 4, 6, 8, 12, and 24 h to obtain blood and lung tissue. Plasma and lung concentrations of delamanid were determined by high-performance liquid chromatographic-tandem mass spectrometry (HPLC-MS/MS), according to the method described by Hirao et al. (19). Plasma  $AUC_{0-24}$  values were calculated by the linear trapezoidal method using Microsoft Excel.

Based on the data from the single-dose PK study, PK parameters from multidose delamanid at 0.625, 2.5, or 10 mg/kg were then simulated by the nonparametric superposition method using Phoenix WinNonlin software, version 6.3, in various 28-day treatment regimens—twice daily, once daily, three times per week, or once per week—the same regimens that were used in the efficacy experiments, as described below (Table 1). Results of these simulations, in combination with the delamanid MIC of 0.012 mg/liter for the *M. tuberculosis* Kurono strain (used in the efficacy study), were used to calculate the following PK/PD indices: weekly (504 to 672 h corresponds to the fourth week of treatment)  $AUC_{504-672}/AUC_{504-672}/MIC$ , daily  $AUC_{504-672}/7$ , daily  $AUC/MIC$ ,  $C_{max504-672}$ ,  $C_{max504-672}/MIC$ , and  $\%T_{>MIC}$ , i.e., percentage of time above MIC during the fourth week of treatment.

**PK/PD index and PDT assessments in mice.** Mice were infected with *M. tuberculosis* Kurono by tail vein injection at  $1.2 \times 10^3$  CFU/mouse. Starting from 4 weeks postinfection (average bacterial load at the time of treatment was  $5.964 \log_{10}$  CFU/lung for 5 mice), the mice were treated with delamanid by oral gavage for 28 days using eight different dosing regimens (Table 1), with five animals per treatment group, except for one group with only four mice due to a technical error (Table 1). One group of mice did not receive delamanid and served as untreated controls. At the end of the 28-day treatment period, mice were sacrificed by exsanguination through the abdominal inferior vena cava under ether anesthesia, and lung tissue was aseptically excised. Dilutions of lung homogenates were plated on 7H11 agar medium supplemented with 10% oleic acid-albumin-dextrose-catalase (OADC), and the plates were incubated at 37°C until colonies were sufficiently grown for visual counting (usually 3 weeks). The  $\log_{10}$  CFU/lung reduction in each animal was calculated by subtracting the  $\log_{10}$  CFU from the mean  $\log_{10}$  CFU of untreated controls.

Correlations between the various PK/PD indices and  $\log_{10}$  CFU/lung reduction were analyzed by Pearson’s or Spearman correlation using SAS software, releases 9.1 and 9.3 (SAS Institute Japan Ltd., Tokyo, Japan). A *P* value less than 0.05 was considered statistically significant. Additionally, corrected Akaike information criterion scores obtained from the inhibitory sigmoid  $E_{max}$  modeling of  $\log_{10}$  CFU/lung reduction versus PK/PD indices were further used to determine the PK/PD index for delamanid.

After the PK/PD index was determined (which is  $AUC_{0-24}/MIC$  for delamanid; see Results), the PDT of delamanid in mice (that is, the  $AUC_{0-24}/MIC$  required for 80% of  $E_{max}$  [ $EC_{80}$ ]) was obtained using inhibitory sigmoid  $E_{max}$  modeling of reduction in  $\log_{10}$  CFU per lung from the average  $\log_{10}$  CFU per lung of untreated mice versus the  $AUC_{0-24}/MIC$  ratios for each treatment group, as follows:

$$\log_{10} \text{ CFU/lung} = \frac{E_{max} \times \left( \frac{AUC_{0-24}}{MIC} \right)^{Hill}}{EC_{50}^{Hill} + \left( \frac{AUC_{0-24}}{MIC} \right)^{Hill}} \quad (1)$$

where  $E_{max}$  was the maximum  $\log_{10}$  CFU/lung reduction from untreated controls,  $AUC_{0-24}$  was the average daily AUC from the last week of the 4-week treatment, MIC was 0.012 mg/liter for the infecting *M. tuberculosis* Kurono strain, and  $EC_{50}$  was the 50%  $AUC_{0-24}/MIC$  ratio for maximum  $\log_{10}$  CFU decline. The  $AUC_{0-24}/MIC$  values corresponding to exposure required for 50% of  $E_{max}$  ( $EC_{50}$ ),  $EC_{80}$ , and  $EC_{90}$  were calculated. These analyses were performed with SAS software, release 9.3 (SAS Institute Japan, Ltd.).

**Pharmacodynamic target assessments in the HFS-TB.** The design of the HFS-TB can be found in previous publications (43, 44) and is described briefly below. The HFS-TB was adapted for delamanid by addition of 0.1% Tween 80 and 10% bovine serum albumin to Middlebrook 7H9 broth. Delamanid concentration was measured by liquid chromatography with tandem mass spectrometry using a Waters (Milford, MA, USA) Acquity UPLC connected to a Waters Xevo TQ mass spectrometer. Data were collected using MassLynx version 4.1 SCN810 software.

Delamanid was infusion based on preliminary HFS PK experiments that identified the corresponding conditions to best mimic human PK parameters, with  $C_{max}$  at 4 h and a terminal half-life of 30 h to match that in humans (30 to 38 h) (7). PK parameters were derived from a one-compartment model, which provided excellent estimation of actual measured concentrations, as shown in Fig. S3. The PK model-derived  $AUC_{0-24}$  at each efficacy sampling day was then obtained for the use in the inhibitory sigmoid  $E_{max}$  model, as described below. Bacterial killing was studied in two *M. tuberculosis* culture conditions: log-phase growth and culture at pH 5.8.

**(i) Log-phase-growth study.** To prepare the inoculum, *M. tuberculosis* H37Rv was grown to log phase in Middlebrook 7H9 broth with 10% OADC for 4 days under shaking conditions and 5%  $CO_2$ . On day 0, 20 ml of  $6 \log_{10}$  CFU/ml culture was inoculated into each hollow-fiber system. Starting on day 1 (average bacterial load was  $6.15 \log_{10}$  CFU/ml), doses of delamanid were administered to achieve the targets described in Table S3. These dose regimens were designed to cover the  $EC_{80}$  identified in the mouse study with sufficient exposures below and above this level to allow the establishment of an exposure-response curve. Different concentrations of delamanid were prepared in a 2-ml volume and infused over 4 h using a syringe pump. Treatment was administered daily for 28 days. The peripheral compartment of each HFS-TB was sampled on study days 3, 7, 10, 14, 21, and 28 to determine the

number of bacterial CFU per milliliter. Samples for PK analysis were collected from each HFS-TB central compartment starting 15 min prior to the day 28 dose (time zero), with time points at 2, 4, 12, 20, 24, 48, and 72 h after the start of the last infusion.

**(ii) *M. tuberculosis* cultured at pH 5.8.** Growth at pH 5.8 was carried out as described for log-phase growth with the following modifications: nonreplicating *M. tuberculosis* strain H37Rv was propagated under acidic conditions (pH 5.8) before being inoculated into the HFS at an inoculum of  $1 \times 10^5$  ( $5 \log_{10}$ ) CFU/ml. At day 1 of treatment initiation, the bacterial load was 5.98  $\log_{10}$  CFU/ml. The target exposures for the pH 5.8 study are shown in Table S4. Two additional exposures higher than those evaluated in the log-phase study were included in the anticipation that higher exposures were needed to kill bacilli cultured at pH 5.8.

**(iii) Efficacy determination.** Quantitative cultures were performed on bacterial samples collected from each HFS-TB peripheral compartment. The samples were obtained just before administration of the next scheduled dose of delamanid. To prevent drug carryover, each 1-ml sample was washed twice, resuspended, and serially diluted 10-fold in sterile saline for quantitative cultures. Each dilution was then cultured on antibiotic-free Middlebrook 7H10 agar plates supplemented with 10% OADC. All cultures were incubated under 5%  $\text{CO}_2$  at 37°C for 21 days for CFU counting.

As in the mouse study, the inhibitory sigmoid  $E_{\text{max}}$  model (equation 1) was used to estimate the  $\text{EC}_{50}$  and  $\text{EC}_{80}$ . The MIC was 0.015 mg/liter for *M. tuberculosis* strain H37Rv,  $E_{\text{max}}$  was maximum bacterial killing from time-matched untreated controls, and the Hill coefficient was estimated for this analysis. S-ADAPT and ADAPT 5 (Biomedical Simulations Resources, University of Southern California) were used for data analysis.

**PDT assessments in trials 101 and 102.** Data from two EBA trials, trial 101 and trial 102 (Table S5), were used to assess the relationship between  $\text{AUC}_{0-24}/\text{MIC}$  and bacterial kill trajectories in humans.  $\text{AUC}_{0-24}/\text{MIC}$  was obtained using the individual daily AUC (trial 101, AUC on day 14; trial 102, AUC on day 7 [calculated by the linear trapezoidal rule with R version 3.2.2]) divided by the MIC for the clinical isolate from the same patient at baseline determined using the proportion method. Bacterial killing was calculated by the reduction of  $\log_{10}$  CFU per milliliter from the baseline to the lowest sputum  $\log_{10}$  CFU per milliliter for the 7-day treatment period in trial 101 and to the day 14  $\log_{10}$  CFU per milliliter in trial 101. The inhibitory sigmoidal  $E_{\text{max}}$  model (as shown in equation 1) and nonlinear mixed-effect analysis were used to model the data. The analysis was performed using NONMEM software, version 7.3.0 (ICON, Dublin, Ireland). Summary statistics and raw data used for the analysis are provided in Tables S6 and S7.

**CFRs for the 100-mg BID and 200-mg QD delamanid doses.** In trial 204, delamanid plasma concentrations were determined predose and 2, 3, 4, 10, 12, 13, 14, and 24 h postdose on days 1, 14, 28, and 56 following administration of delamanid at 100 mg BID in MDR-TB patients. Daily AUCs on days 1, 14, 28, and 56 were determined by noncompartmental analysis (NCA) methods. The average steady-state  $\text{AUC}_{0-24}$  was determined by averaging the  $\text{AUC}_{0-24}$  on days 14, 28, and 56. In trial 213, patients received 100 mg delamanid BID plus OBR for 2 months, followed by 200 mg delamanid QD plus OBR for 4 months. Due to sparse sampling of the PK in this study, the steady-state  $\text{AUC}_{0-24}$  values following the 100-mg BID and 200-mg QD dosing were estimated based on a population PK model (30). Baseline MICs for *M. tuberculosis* isolates from each patient were determined using the proportion method (4). Patients with *M. tuberculosis* isolates that had baseline MICs of  $\leq 0.016$  mg/liter were included in the analyses, as this MIC has been established as the critical concentration for delamanid (45). The calculated individual  $\text{AUC}_{0-24}/\text{MIC}$  values from trial 204 and trial 213 were compared with the selected PDT values (mouse, HFS-TB plasma-equivalent, and human EBA PDTs) to determine the CFR.

**QTc interval determination.** In trial 213, 12-lead electrocardiograms (ECG) were recorded at screening baseline (day -1), at day 1, and at weekly visits from week 1 to week 12 and biweekly from week 14 to 26 during the 6-month treatment, with the subject supine and at rest for at least 10 min. During treatment, three ECGs were collected 5 to 10 min apart after the morning dose of IMP (investigational medicinal product). In addition to the initial clinical interpretation for ongoing safety evaluation by the investigator, digitally acquired ECGs were received by the central reader for processing and were analyzed by a central reader. QT intervals were corrected for heart rate using Fridericia's formula (QTcF) and averaged from the 3 ECG readings. Delamanid's QTc prolongation effect is mainly caused by one of its metabolites, DM-6705 (7), as DM-6705 concentrations were identified as a surrogate marker for QTc prolongation. The terminal half-life of DM-6705 is about 10 days; thus, plasma concentrations of this metabolite fluctuate very little at steady state, which is reached in about 7 weeks. Hence, the timing of performing ECGs, at or beyond 7 weeks, is not important to determine the effect of delamanid on QTc.

## SUPPLEMENTAL MATERIAL

Supplemental material is available online only.

**SUPPLEMENTAL FILE 1**, PDF file, 0.6 MB.

## ACKNOWLEDGMENTS

We acknowledge and thank the patients and investigators who participated in the clinical trials discussed herein.

The HFS-TB study was supported by the Critical Path to TB Drug Regimens Initiative, a partnership between the Bill and Melinda Gates Foundation and the Critical Path Institute (Tucson, AZ, USA). The rest of the studies in this report were supported by

Otsuka Pharmaceutical Development & Commercialization, Inc., Rockville, MD, USA (OPDC), and Otsuka Pharmaceutical Co., Ltd., Tokushima, Japan (OPC). David Norris (Ecosse Medical Communications, Falmouth, MA, USA) provided editorial services during the writing of the manuscript; these editorial services were supported by OPDC.

## REFERENCES

- World Health Organization. 2019. Global tuberculosis report 2019. <https://apps.who.int/iris/bitstream/handle/10665/329368/9789241565714-eng.pdf?ua=1>. Accessed January 2020.
- Matsumoto M, Hashizume H, Tomishige T, Kawasaki M, Tsubouchi H, Sasaki H, Shimokawa Y, Komatsu M. 2006. OPC-67683, a nitro-dihydroimidazo[4,5-b]pyridine derivative with promising action against tuberculosis in vitro and in mice. *PLoS Med* 3:e466. <https://doi.org/10.1371/journal.pmed.0030466>.
- Nataraj V, Varela C, Javid A, Singh A, Besra GS, Bhatt A. 2015. Mycolic acids: deciphering and targeting the Achilles' heel of the tubercle bacillus. *Mol Microbiol* 98:7–16. <https://doi.org/10.1111/mmi.13101>.
- Stinson K, Kurepina N, Venter A, Fujiwara M, Kawasaki M, Timm J, Shashkina E, Kreiswirth BN, Liu Y, Matsumoto M, Geiter L. 2016. MIC of delamanid (OPC-67683) against Mycobacterium tuberculosis clinical isolates and a proposed critical concentration. *Antimicrob Agents Chemother* 60:3316–3322. <https://doi.org/10.1128/AAC.03014-15>.
- Gler MT, Skripconoka V, Sanchez-Garavito E, Xiao H, Cabrera-Rivero JL, Vargas-Vasquez DE, Gao M, Awad M, Park SK, Shim TS, Suh GY, Danilovits M, Ogata H, Kurve A, Chang J, Suzuki K, Tupasi T, Koh WJ, Seaworth B, Geiter LJ, Wells CD. 2012. Delamanid for multidrug-resistant pulmonary tuberculosis. *N Engl J Med* 366:2151–2160. <https://doi.org/10.1056/NEJMoa1112433>.
- von Groote-Bidlingmaier F, Patientia R, Sanchez E, Balanag V, Jr, Ticona E, Segura P, Cadena E, Yu C, Cirule A, Lizarbe V, Davidaviciene E, Domente L, Variava E, Caoili J, Danilovits M, Bielskiene V, Staples S, Hittel N, Petersen C, Wells C, Hafkin J, Geiter LJ, Gupta R. 2019. Efficacy and safety of delamanid in combination with an optimised background regimen for treatment of multidrug-resistant tuberculosis: a multicentre, randomised, double-blind, placebo-controlled, parallel group phase 3 trial. *Lancet Respir Med* 7:249–259. [https://doi.org/10.1016/S2213-2600\(18\)30426-0](https://doi.org/10.1016/S2213-2600(18)30426-0).
- European Medicines Agency. 2020. Delytba European public assessment report (EPAR). [https://www.ema.europa.eu/en/documents/assessment-report/delytba-epar-public-assessment-report\\_en.pdf](https://www.ema.europa.eu/en/documents/assessment-report/delytba-epar-public-assessment-report_en.pdf). Accessed September 2020.
- World Health Organization. 2016. The use of delamanid in the treatment of multidrug-resistant tuberculosis in children and adults: interim policy guidance. <https://www.ncbi.nlm.nih.gov/books/NBK396145/>. Accessed February 2020.
- Gupta R, Geiter LJ, Wells CD, Gao M, Cirule A, Xiao H. 2015. Delamanid for extensively drug-resistant tuberculosis. *N Engl J Med* 373:291–292. <https://doi.org/10.1056/NEJMc1415332>.
- Skripconoka V, Danilovits M, Pehme L, Tomson T, Skenders G, Kummik T, Cirule A, Leimane V, Kurve A, Levina K, Geiter LJ, Manissero D, Wells CD. 2013. Delamanid improves outcomes and reduces mortality in multidrug-resistant tuberculosis. *Eur Respir J* 41:1393–1400. <https://doi.org/10.1183/09031936.00125812>.
- Wells CD, Gupta R, Hittel N, Geiter LJ. 2015. Long-term mortality assessment of multidrug-resistant tuberculosis patients treated with delamanid. *Eur Respir J* 45:1498–1501. <https://doi.org/10.1183/09031936.00176314>.
- Gumbo T, Pasipanodya JG, Romero K, Hanna D, Nuermberger E. 2015. Forecasting accuracy of the hollow fiber model of tuberculosis for clinical therapeutic outcomes. *Clin Infect Dis* 61(Suppl 1):S25–S31. <https://doi.org/10.1093/cid/civ427>.
- Tuntland T, Ethell B, Kosaka T, Blasco F, Zang RX, Jain M, Gould T, Hoffmaster K. 2014. Implementation of pharmacokinetic and pharmacodynamic strategies in early research phases of drug discovery and development at Novartis Institute of Biomedical Research. *Front Pharmacol* 5:174. <https://doi.org/10.3389/fphar.2014.00174>.
- Srivastava S, Magombedze G, Koeth T, Sherman C, Pasipanodya JG, Raj P, Wakeland E, Deshpande D, Gumbo T. 2017. Linezolid dose that maximizes sterilizing effect while minimizing toxicity and resistance emergence for tuberculosis. *Antimicrob Agents Chemother* 61:e00751-17. <https://doi.org/10.1128/AAC.00751-17>.
- Deshpande D, Srivastava S, Pasipanodya JG, Bush SJ, Nuermberger E, Swaminathan S, Gumbo T. 2016. Linezolid for infants and toddlers with disseminated tuberculosis: first steps. *Clin Infect Dis* 63:S80–S87. <https://doi.org/10.1093/cid/ciw482>.
- Modongo C, Pasipanodya JG, Magazi BT, Srivastava S, Zetola NM, Williams SM, Sirugo G, Gumbo T. 2016. Artificial intelligence and amikacin exposures predictive of outcomes in multidrug-resistant tuberculosis patients. *Antimicrob Agents Chemother* 60:5928–5932. <https://doi.org/10.1128/AAC.00962-16>.
- Drusano GL, Sgambati N, Eichas A, Brown DL, Kulawy R, Louie A. 2010. The combination of rifampin plus moxifloxacin is synergistic for suppression of resistance but antagonistic for cell kill of Mycobacterium tuberculosis as determined in a hollow-fiber infection model. *mBio* 1:e00139-10. <https://doi.org/10.1128/mBio.00139-10>.
- Gumbo T, Louie A, Liu W, Ambrose PG, Bhavnani SM, Brown D, Drusano GL. 2007. Isoniazid's bactericidal activity ceases because of the emergence of resistance, not depletion of Mycobacterium tuberculosis in the log phase of growth. *J Infect Dis* 195:194–201. <https://doi.org/10.1086/510247>.
- Hirao Y, Koga T, Koyama N, Shimokawa Y, Umehara K. 2015. Liquid chromatography-tandem mass spectrometry methods for determination of delamanid in mouse plasma and lung. *Am J Anal Chem* 6:98–105. <https://doi.org/10.4236/ajac.2015.62009>.
- Ordenez AA, Wang H, Magombedze G, Ruiz-Bedoya CA, Srivastava S, Chen A, Tucker EW, Urbanowski ME, Pieterse L, Fabian Cardozo E, Lodge MA, Shah MR, Holt DP, Mathews WB, Dannals RF, Gobburu JVS, Peloquin CA, Rowe SP, Gumbo T, Ivaturi VD, Jain SK. 2020. Dynamic imaging in patients with tuberculosis reveals heterogeneous drug exposures in pulmonary lesions. *Nat Med* 26:529–534. <https://doi.org/10.1038/s41591-020-0770-2>.
- Dheda K, Lenders L, Magombedze G, Srivastava S, Raj P, Arning E, Ashcraft P, Bottiglieri T, Wainwright H, Pennel T, Linegar A, Moodley L, Pooran A, Pasipanodya JG, Sirgel FA, van Helden PD, Wakeland E, Warren RM, Gumbo T. 2018. Drug-penetration gradients associated with acquired drug resistance in patients with tuberculosis. *Am J Respir Crit Care Med* 198:1208–1219. <https://doi.org/10.1164/rccm.201711-2333OC>.
- Liu Y, Matsumoto M, Ishida H, Ohguro K, Yoshitake M, Gupta R, Geiter L, Hafkin J. 2018. Delamanid: from discovery to its use for pulmonary multidrug-resistant tuberculosis (MDR-TB). *Tuberculosis (Edinb)* 111:20–30. <https://doi.org/10.1016/j.tube.2018.04.008>.
- Diacon AH, Dawson R, Hanekom M, Narunsky K, Venter A, Hittel N, Geiter LJ, Wells CD, Paccaly AJ, Donald PR. 2011. Early bactericidal activity of delamanid (OPC-67683) in smear-positive pulmonary tuberculosis patients. *Int J Tuberc Lung Dis* 15:949–954. <https://doi.org/10.5588/ijtld.10.0616>.
- European Medicines Agency Committee for Medicinal Products for Human Use. 2016. Guideline on the use of pharmacokinetics and pharmacodynamics in the development of antimicrobial medicinal products. European Medicines Agency, London, United Kingdom.
- Center for Drug Evaluation and Research. 2018. Microbiology data for systemic antibacterial drugs—development, analysis, and presentation. <https://www.fda.gov/media/77442/download>. Accessed September 2020.
- World Health Organization. 2018. Technical report on the pharmacokinetics and pharmacodynamics (PK/PD) of medicines used in the treatment of drug-resistant tuberculosis. <https://apps.who.int/iris/bitstream/handle/10665/260440/WHO-CDS-TB-2018.6-eng.pdf?sequence=1&isAllowed=y>. Accessed September 2020.
- Cavaleri M, Manolis E. 2015. Hollow fiber system model for tuberculosis: the European Medicines Agency experience. *Clin Infect Dis* 61(Suppl 1):S1–S4. <https://doi.org/10.1093/cid/civ484>.
- Romero K, Clay R, Hanna D. 2015. Strategic regulatory evaluation and endorsement of the hollow fiber tuberculosis system as a novel drug development tool. *Clin Infect Dis* 61(Suppl 1):S5–S9. <https://doi.org/10.1093/cid/civ424>.
- Chilukuri D, McMaster O, Bergman K, Colangelo P, Snow K, Toerner JG.

2015. The hollow fiber system model in the nonclinical evaluation of antituberculosis drug regimens. *Clin Infect Dis* 61(Suppl 1):S32–S33. <https://doi.org/10.1093/cid/civ460>.
30. Wang X, Mallikaarjun S, Gibiansky E. 2021. Population pharmacokinetic analysis of delamanid in patients with pulmonary multidrug-resistant tuberculosis. *Antimicrob Agents Chemother* 65:e01202-20. <https://doi.org/10.1128/AAC.01202-20>.
31. Gumbo T, Angulo-Barturen I, Ferrer-Bazaga S. 2015. Pharmacokinetic-pharmacodynamic and dose-response relationships of antituberculosis drugs: recommendations and standards for industry and academia. *J Infect Dis* 211(Suppl 3):S96–S106. <https://doi.org/10.1093/infdis/jiu610>.
32. Pasipanodya J, Gumbo T. 2011. An oracle: antituberculosis pharmacokinetics-pharmacodynamics, clinical correlation, and clinical trial simulations to predict the future. *Antimicrob Agents Chemother* 55:24–34. <https://doi.org/10.1128/AAC.00749-10>.
33. Simner PJ, Miller L. 2018. Understanding pharmacokinetics (PK) and pharmacodynamics (PD). [https://clsi.org/media/1990/ast\\_news\\_update\\_jan18-pkpd.pdf](https://clsi.org/media/1990/ast_news_update_jan18-pkpd.pdf). Accessed September 2020.
34. National Institute of Allergy and Infectious Diseases. 2017. NIAID Workshop 'Pharmacokinetics-Pharmacodynamics (PKPD) for Development of Therapeutics against Bacterial Pathogens', June 14–15, 2017, Bethesda, MD. [http://amr.solutions/wp-content/uploads/99/niaid\\_june2017\\_pkpdworkshopsummary.pdf](http://amr.solutions/wp-content/uploads/99/niaid_june2017_pkpdworkshopsummary.pdf). Accessed September 2020.
35. Institute for Clinical Pharmacodynamics. 2017. De-risking antibiotic drug development with PK-PD. <http://icpd.com/downloads/ICPD-White-Paper-De-risking-Drug-Development-with-PK-PD.pdf>. Accessed September 2020.
36. Srivastava S, Pasipanodya JG, Gumbo T. 2017. pH conditions under which pyrazinamide works in humans. *Antimicrob Agents Chemother* 61:e00854-17. <https://doi.org/10.1128/AAC.00854-17>.
37. Kempker RR, Heinrichs MT, Nikolaishvili K, Sabulua I, Bablshvili N, Gogishvili S, Avaliani Z, Tukvadze N, Little B, Bernheim A, Read TD, Guarner J, Derendorf H, Peloquin CA, Blumberg HM, Vashakidze S. 2017. Lung tissue concentrations of pyrazinamide among patients with drug-resistant pulmonary tuberculosis. *Antimicrob Agents Chemother* 61:e00226-17. <https://doi.org/10.1128/AAC.00226-17>.
38. McDermott W, Tompsett R. 1954. Activation of pyrazinamide and nicotinamide in acidic environments in vitro. *Am Rev Tuberc* 70:748–754. <https://doi.org/10.1164/art.1954.70.4.748>.
39. McCune RM, Feldmann FM, Lambert HP, McDermott W. 1966. Microbial persistence. I. The capacity of tubercle bacilli to survive sterilization in mouse tissues. *J Exp Med* 123:445–468. <https://doi.org/10.1084/jem.123.3.445>.
40. Mitchison DA. 1979. Basic mechanisms of chemotherapy. *Chest* 76:771–781. [https://doi.org/10.1378/chest.76.6\\_supplement.771](https://doi.org/10.1378/chest.76.6_supplement.771).
41. Chen X, Hashizume H, Tomishige T, Nakamura I, Matsuba M, Fujiwara M, Kitamoto R, Hanaki E, Ohba Y, Matsumoto M. 2017. Delamanid kills dormant Mycobacteria in vitro and in a guinea pig model of tuberculosis. *Antimicrob Agents Chemother* 61:e02402-16. <https://doi.org/10.1128/AAC.02402-16>.
42. Strydom N, Gupta SV, Fox WS, Via LE, Bang H, Lee M, Eum S, Shim T, Barry CE, III, Zimmerman M, Dartois V, Savic RM. 2019. Tuberculosis drugs' distribution and emergence of resistance in patient's lung lesions: a mechanistic model and tool for regimen and dose optimization. *PLoS Med* 16:e1002773. <https://doi.org/10.1371/journal.pmed.1002773>.
43. European Medicines Agency. 2015. In-vitro hollow fiber system model of tuberculosis (HSF-TB). [https://www.ema.europa.eu/en/documents/regulatory-procedural-guideline/qualification-opinion-vitro-hollow-fibre-system-model-tuberculosis-hfs-tb\\_en.pdf](https://www.ema.europa.eu/en/documents/regulatory-procedural-guideline/qualification-opinion-vitro-hollow-fibre-system-model-tuberculosis-hfs-tb_en.pdf). Accessed September 2019.
44. Srivastava S, Gumbo T. 2011. In vitro and in vivo modeling of tuberculosis drugs and its impact on optimization of doses and regimens. *Curr Pharm Des* 17:2881–2888. <https://doi.org/10.2174/138161211797470192>.
45. World Health Organization. 2018. Technical report on critical concentrations for drug susceptibility testing of medicines used in the treatment of drug-resistant tuberculosis. [https://www.who.int/tb/publications/2018/WHO\\_technical\\_report\\_concentrations\\_TB\\_drug\\_susceptibility/en/](https://www.who.int/tb/publications/2018/WHO_technical_report_concentrations_TB_drug_susceptibility/en/). Accessed September 2019.